2016 Eleventh International Conference on Ecological Vehicles and Renewable Energies (EVER)

Frequency-Domain Homogenization for Impedance Characterization of Litz-Wire Transformers in 2-D Finite Element Models

Korawich Niyomsatian*‡ Jeroen Van den Keybus* Ruth V. Sabariego† Johan Gyselinck‡

*Triphase NV
Romeinse straat 18,
3001 Heverlee, Belgium
korawich.niyomsatian@triphase.com
jeroenvandenkeybus@triphase.com

†KU Leuven
Leuven, Belgium
ruth.sabariego@esat.kuleuven.be

‡Université Libre de Bruxelles
BEAM Department
50, Av. F. Roosevelt, B-1050, Brussels
johan.gyselinck@ulb.ac.be

***Abstract*—This work deals with a frequency-domain homogenization technique for litz-wire bundles in transformers. The approach consists in adopting a frequency-dependent complex reluctivity in the litz-wire bundles and a frequency-dependent complex impedance in the electrical circuit. The litz-wire bundles become homogeneous conductors which are easy to integrate into a finite element model of a transformer. The magnetic flux and the impedance of the litz-wire transformer computed from the homogenized model agree well with the reference fine model in which each litz-wire turn is finely discretized. The errors of the computed resistance and inductance values are less than 3% and 0.03% respectively with several times faster calculation.**

Keywords*—*litz wire; complex impedance; complex permeability; high-frequency transformer; skin effect; proximity effect; homogenization; finite element analysis.

I. Introduction

Nowadays power converters are able to operate at higher frequencies thanks to the advent of wide-bandgap semiconductor devices. Accordingly, litz wire has become the more important element because it allows reducing the skin-effect losses at high frequencies thanks to the small strands connected in parallel as a bundle instead of using one big strand as shown in Fig. 1. The applications range from small switched mode power supplies to high-power solid-state transformers [1].

Although the proper twisting or weaving of the strands in a litz-wire bundle ensures that the current flowing in each strand is almost equal, the losses in litz wire can still be excessively dominated by proximity-effect losses at the strand level [2]. To minimize the eddy-current losses in litz wire one may reduce the diameter of the strand while increasing the number of strands to maintain the same copper area for the same current rating, however, at the expense of increased cost and resistance, and reduced fill factor [3]. Also the soft-switching algorithms relying on the inductance of transformers are widely used for power converters to achieve better efficiency and power density. This indicates that accurately predicting the impedance of the litz wire is important. Some analytical formulas have been published in [4], but they are not always accurate in some practical cases [5]. On the other hand, finite element analysis (FEA) allows for higher accuracy as well as for more modeling flexibility (e.g. including the creepage distance between each winding).

However, to capture the skin and proximity effect, the characteristic length of the FE discretization of the conductors should be at least three times smaller than the skin depth as a rule of thumb. This amounts to a huge number of unknowns and prohibitive computational cost and it is thus not suitable for the design process, particularly when the number of strands drastically increases in high-power applications. Thanks to the homogenization method, a litz-wire bundle is replaced by a round homogeneous conductor as depicted in Fig. 1, which is easy to integrate into a finite element model of a transformer.

The objective of this work is to adapt and apply the homogenization technique in [6], which has proved successful for multi-turn-winding inductors in [6],[7] to the impedance characterization of litz-wire transformers. Although there have been several authors publishing similar works on this topic, in [8],[9], they focus only on either square or hexagonally packed conductors, and the

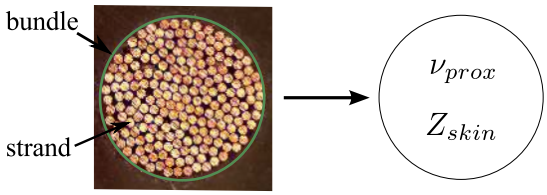

Fig. 1. Micrograph of cross-section of a real 0.1-mm-diameter 200-strand litz-wire bundle with $\lambda = 0.4$ (left) being homogenized with complex, frequency-dependent, fill-factor-dependent reluctivity and impedance (right).

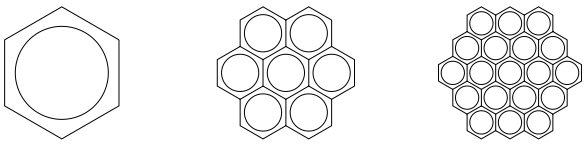

(a) $n_{layer} = 0$ (b) $n_{layer} = 1$ (c) $n_{layer} = 2$

Fig. 2. Representative model with different number of layers around the central cell.

method proposed in [5] is not implemented explicitly in terms of the fill factor of the litz-wire bundle, neither the skin-effect impedance is included. In this work, these two types of regular packings are considered and compared.

II. Frequency-domain characterization of litz-wire bundles

According to [6], a complete eddy-current effect characterization of the strand conductors and their packing inside the litz-wire bundle can be carried out by means of a representative 2-D FE model consisting of a central cell and a number of layers n_{layer} around, of which the effect will be illustrated in the following subsection. Fig. 2 shows the representative models with different number of layers for the case of hexagonal packing. Each elementary cell comprises the cross-section of one conductor, where the skin and proximity effects occur, and the surrounding insulation.

Moreover, with this method, one can choose the arrangement of these cells depending on the packing. In general, there are two types of regular packing of round conductors in a winding: square and hexagonal. It can be observed in Fig. 1 that the configuration of the strands inside the bundle is not well organized, but some parts can be noticed as a hexagonal packing (mostly in the dense area). It can probably be said that the practical litz wire is a combination of these two ideal packing patterns [5]. Initially, in this section, we consider both of the square and hexagonally packed strands as the representative model as displayed in Figs. 3 and 4 respectively.

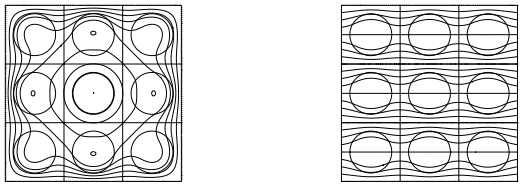

Fig. 3. Representative model of square packed strand conductors of $\lambda = 0.4$ with elementary flux pattern for skin-effect (left) and proximity-effect (right) at $X = 2$.

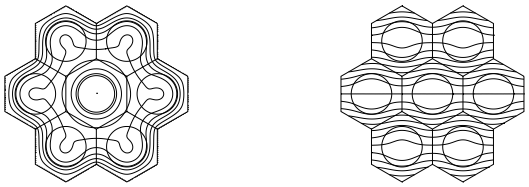

Fig. 4. Representative model of hexagonally packed strand conductors of $\lambda = 0.4$ with elementary flux pattern for skin-effect (left) and proximity-effect (right) at $X = 2$.

The frequency-domain 2-D FE calculations in this paper are carried out using the classical magnetic vector potential $(a-)$formulation with complex notation for the sinusoidal time variation ($\mathbf{i}$ is imaginary unit and the time derivative is replaced by $\mathbf{i}\omega$). The skin depth at frequency f or pulsation $\omega = 2\pi f$ is given by $\delta = \sqrt{2/(\sigma\omega\mu_0)}$, where σ is the conductivity of the conductors and μ_0 H/m their permeability (or ν_0 reluctivity). The normalized or *reduced frequency* X is defined as:

$$X = r_s/\delta = \sqrt{f} \cdot r_s\sqrt{\pi\sigma\mu_0} \tag{1}$$

with r_s the nominal radius of the litz-wire strand. Another important parameter for the representative model is the fill factor of a bundle $\lambda = n(r_s/r_b)^2$ where r_b is the radius of a litz-wire bundle and n the number of strands in the bundle.

The skin and proximity effects are characterized in the form of a lumped frequency-dependent complex impedance $Z_{skin}(X)$ and a frequency-dependent complex reluctivity $\nu_{prox}(X)$ respectively by using this representative model. Thanks to the spatial orthogonality, the skin and proximity effect are decoupled. The skin-effect impedance is computed by imposing a unit current in each wire by means of electrical circuit equations. The proximity-effect reluctivity is obtained by imposing a unit average flux density by means of the following boundary condition [6]:

$$a(x,y)|_{\partial\Omega} = yB'_x - xB'_y \tag{2}$$

where B'_x and B'_y are the components of the average magnetic flux density vector in the domain Ω. Figs. 3 and 4 show the resultant flux lines in the square- and hexagonal-packing representative models excited by the explained procedure. Subsequently the complex power absorbed by the central cell is computed from

$$S = P + \mathbf{i}Q = \frac{l}{2}\int_{\Omega_{central}} (j^2/\sigma + \mathbf{i}\omega b^2/\mu_0)\, d\Omega \quad (3)$$

where P and Q are the active and reactive powers respectively, j^2 and b^2 the r.m.s.-value squared of the current density and flux density respectively and l the length along the third dimension (z-axis). The skin-effect frequency-dependent impedance can be written in terms of the dimensionless coefficients p_I and q_I as [6]

$$\begin{aligned} Z_{skin} &= p_I(X)R_{dc} + \mathbf{i}\omega q_I(X)\frac{\mu_0 l}{8\pi\lambda} \\ &= R_{dc}\left(p_I(X) + \mathbf{i}q_I(X)\frac{X^2}{4\lambda}\right) \end{aligned} \quad (4)$$

where $R_{dc} = l/(\sigma\pi r_s^2)$ is the DC resistance of the conductor and $\mu_0 l/(8\pi)$ the internal DC inductance of a round conductor with length l. Thus the coefficients p_I and q_I follow directly from P and Q values respectively. Analogously, for the proximity-effect, the frequency-dependent complex reluctivity can be written in terms of the dimensionless coefficients p_B and q_B as

$$\begin{aligned} \nu_{prox} &= \nu_0 q_B(X) + \mathbf{i}p_B(X)\frac{1}{4}\lambda\sigma r_s^2\omega \\ &= \nu_0\left(q_B(X) + \mathbf{i}p_B(X)\frac{\lambda X^2}{4}\right) \end{aligned} \quad (5)$$

where the factor $\lambda\sigma r_s^2\omega/4$ follows from the analytical expression for low-frequency proximity losses in a round conductor [8].

A. *The effect of the number of layers n_{layer}*

To examine the effect of the number of layers n_{layer} on the precision of the skin- and proximity-effect coefficients, we compute the coefficients from the representative model with $n_{layer} = 0, 1, 2$ for both square and hexagonally packed round conductors and different values of fill factor λ.

According to Fig. 5, the precision of the computed coefficients from using $n_{layer} = 1, 2$ is good. However the deviation of the skin-effect coefficient q_I can be clearly seen when using $n_{layer} = 0$ at low frequencies for both kinds of packing. The deviations are up to 4% and 15% relative to the values when using $n_{layer} = 1$ in hexagonal-packing and square-packing respectively whereas for the case $n_{layer} = 2$ they are only up to 0.5%

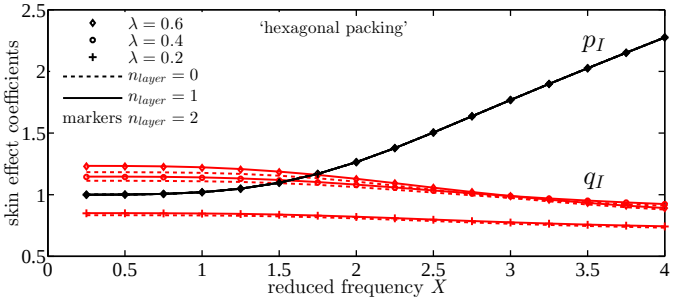

(a) skin effect coefficients

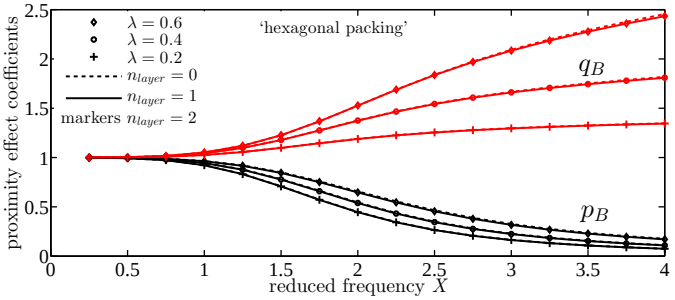

(b) proximity effect coefficients

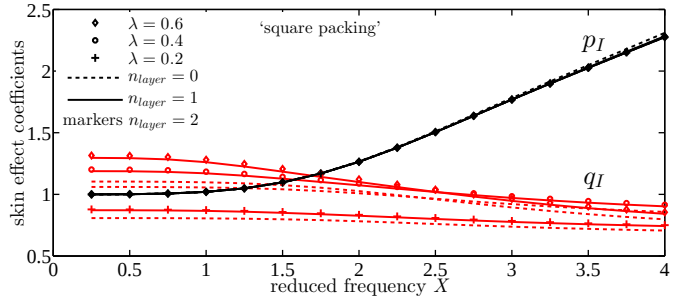

(c) skin effect coefficients

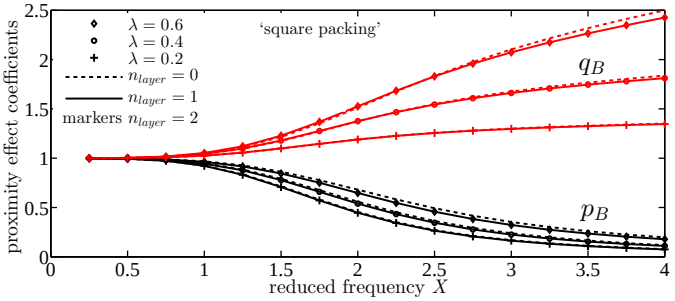

(d) proxmity effect coefficients

Fig. 5. Defined coefficients (p_I, p_B in black and q_I, q_B in red) obtained with the hexagonal- and square-packing representative models for different numbers of the layers around the central cell n_{layer} and different fill factors λ.

and 1.7% relative to the values when using $n_{layer} = 1$. At higher frequencies and high fill factors, the deviations of p_B and q_B of $n_{layer} = 0$ become more clearer. The deviations of those are up to 1% and 3% relative to the values when using $n_{layer} = 1$ in hexagonal-packing and square-packing respectively whereas for the case $n_{layer} = 2$ the deviations are negligible. Hereinafter, the

coefficients of the representative model with $n_{layer} = 1$ will be used.

B. The effect of the packing pattern

For convenience, the skin- and proximity-effect coffcients for homogenization are obtained from the regular-packing representative model: either square or hexagonal. In this section, we study the effect of the packing pattern on these coefficients with $n_{layer} = 1$.

Fig. 6 shows the results of the defined coefficients versus reduced frequency for different fill factors λ. The skin-effect losses and the corresponding coefficient are practically independent of the fill factor λ and when the frequency is sufficiently low, i.e. $X \to 0$, the coefficients p_I and q_B, corresponding to the low-frequency values R_{dc} and ν_0, tend to 1 as expected.

Fig. 6 also shows that in this range of reduced frequency, in which litz wire is commonly used, the difference of cell packing does not cause significant difference in effective complex reluctivity and impedance of a litz-wire bundle at the same fill factor. There are some discrepancies in q_I particularly at high fill factors. The errors is up to 6% at $\lambda = 0.6$ relative to the values from hexagonal-packing model. Nevertheless, the reactive power corresponding to this skin-effect term is usually negligible compared to one corresponding to proximity-effect term in multi-winding applications [6]. Hereinafter, the coefficients of the hexagonally packed conductors will be used.

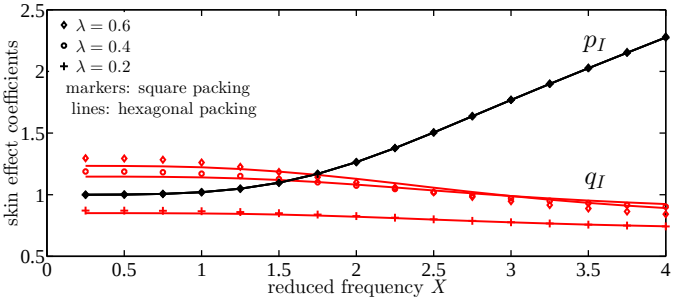

(a) skin effect coefficients

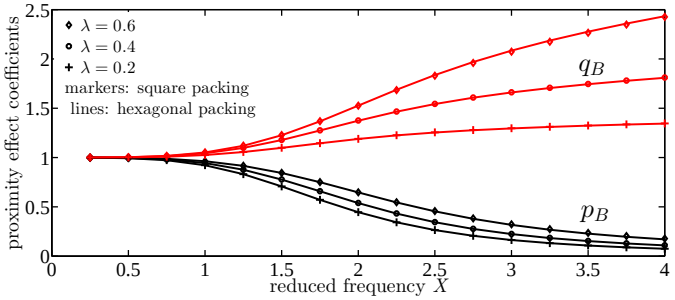

(b) proximity effect coefficients

Fig. 6. Defined coefficients (p_I, p_B in black and q_I, q_B in red) obtained with square packing (markers) and hexagonal packing (lines) representative models with $n_{layer} = 1$ for different fill factors λ.

III. Application to Litz-Wire Transformer Winding

To validate the homogenization approach, the homogenized model is used to compute the impedances of a transformer with litz-wire windings compared with the results computed with the model which is finely discretized as a reference.

The 2-D FE calculations are performed with the open-source programs Gmsh [10] and GetDP [11]. The transformer has translational symmetry along z-axis (into the page). The primary winding has 4 turns of litz-wire bundles (200 strands, $r_s = 0.2\,\mathrm{mm}$, $\lambda = 0.43$, $R_{dc} = 0.66\,\mathrm{m\Omega}$). It is sandwiched by 12 turns of series-connected secondary litz-wire bundles (100 strands, $r_s = 0.2\,\mathrm{mm}$, $\lambda = 0.63$, $R_{dc} = 3.9\,\mathrm{m\Omega}$). The current in each strand is assumed to be equal. Also the core is assumed to be linear and lossless (relative permeability = 1800).

The homogenization method will be applied to the litz-wire bundles using the Z_{skin} and ν_{prox} in (4) and (5) based on the computed coefficients. Each litz-wire bundle becomes a homogeneous conductor with the same diameter as the bundle in which the current density is uniform as shown in Fig. 7. A fine actual model containg small strands for validation is drawn based on the results for circle packing in [12]. To emphasize the benefit of the homogenized model, each of the strands inside the litz-wire bundles is finely discretized in the fine model, leading to a total of 413,600 real unknowns at $X = 2$ ($f = 2.32\,\mathrm{MHz}$), whereas the discretization of the litz-wire bundles is much coarser in the homogenized model, resulting in 16 times less unknowns, viz 25,370.

A. General transformer model in the frequency domain

In the frequency domain, the relation between the terminal phasor voltages v_1 and v_2 and the terminal phasor currents i_1 and i_2 for a two-winding transformer reads [13]:

$$\left.\begin{aligned} v_1 &= (\mathbf{i}\omega L_1 + R_1)i_1 + (\mathbf{i}\omega M + R_M)i_2 \\ v_2 &= (\mathbf{i}\omega M + R_M)i_1 + (\mathbf{i}\omega L_2 + M)i_2 \end{aligned}\right\} \quad (6)$$

where L_1, L_2 and M are the self- and mutual inductances of the windings respectively, and R_1, R_2 and R_M the self- and mutual resistances respectively.

The computation of self-impedance is done by exciting only either primary or secondary winding. The

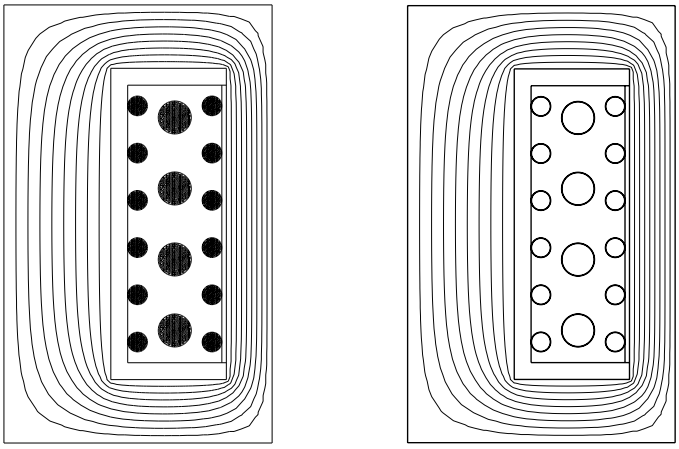

(a) Fine model (b) Homogenized model

Fig. 7. 2D model of the transformer showing the flux lines when only either secondary or primary winding is excited at $X = 2$.

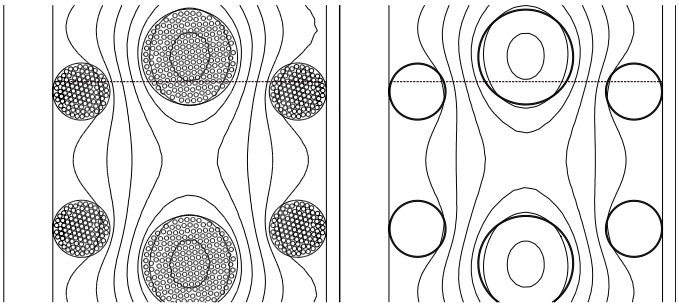

(a) Fine model (b) Homogenized model

Fig. 8. Flux lines when the secondary and the primary currents induce the flux in the magnetic core in the opposite direction and its ratio equals to the turn ratio, at $X = 2$.

computation of mutal-impedance is done by exciting the primary and secondary windings such that the ratio of the currents is turn-ratio but opposite direction. These parameters can be calculated from the following sets of formulas where k is conventionally chosen to be the turn-ratio (the ratio between the numbers of primary and secondary turns):

$$L_1 = \left.\frac{2Q}{i_1 i_1^*}\right|_{i_2=0} \tag{7}$$

$$R_1 = \left.\frac{2P}{i_1 i_1^*}\right|_{i_2=0} \tag{8}$$

$$L_2 = \left.\frac{2Q}{i_2 i_2^*}\right|_{i_1=0} \tag{9}$$

$$R_2 = \left.\frac{2P}{i_2 i_2^*}\right|_{i_1=0} \tag{10}$$

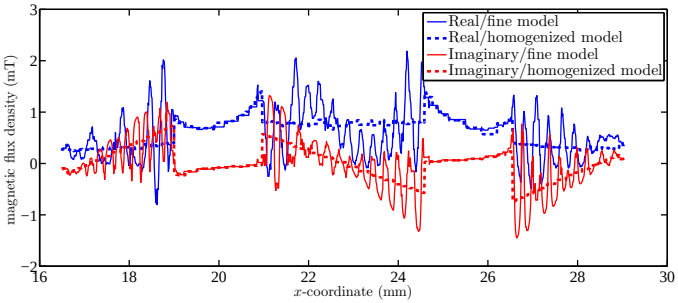

(a) x-component

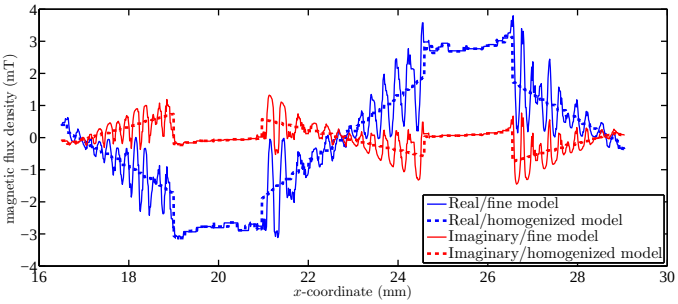

(b) y-component

Fig. 9. Magnetic flux density in the winding window along the dashed-line in Fig. 8 at $X = 2$ ($f = 2.32\,\mathrm{MHz}$).

$$M = \frac{1}{2k}\left(L_1 + k^2 L_2 - \frac{2Q}{i_1 i_1^*}\right)\Bigg|_{i_2=-k i_1} \tag{11}$$

$$R_M = \frac{1}{2k}\left(R_1 + k^2 R_2 - \frac{2P}{i_1 i_1^*}\right)\Bigg|_{i_2=-k i_1} \tag{12}$$

B. Results

The transformer windings in the model are excited correspondingly to (7)-(12) to characterize the impedance. Some computed flux lines at $X = 2$ ($f = 2.32\,\mathrm{MHz}$) are shown in Figs. 7 and 8 for both cases in both fine and homogenized models. In Fig. 7, the flux lines mainly reside in the core when either primary or secondary winding is excited (open-circuit condition). However, when the windings are excited in opposite direction and the ratio of the currents is turn-ratio (short-circuit condition), there is little flux in the core and flux lines in the winding window become more significant as displayed in Fig 8.

Fig. 9 shows the horizontal and vertical components of the complex magnetic flux density along the horizontal dashed line in the winding window in Fig. 8. The flux density obtained with the fine model clearly shows the fluctuation due to the individual conductors located on the line or adjacent to it, whereas the homogenized model does not provide these details. Also it can be seen that the 2-D magnetic field is present in the winding region,

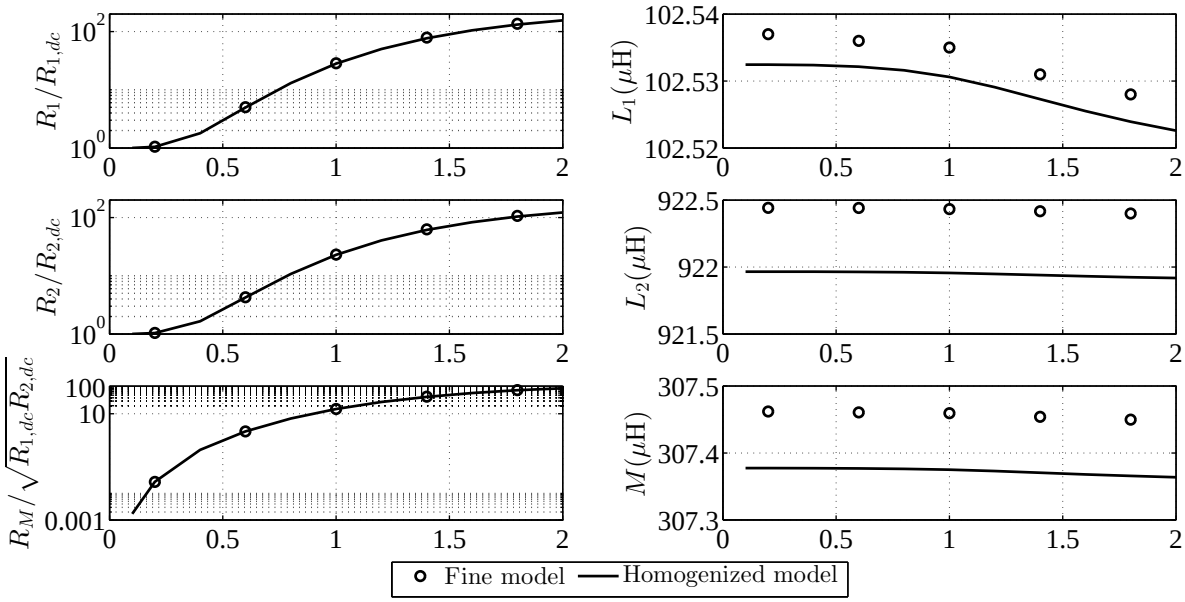

Fig. 10. Self- and mutual normalized resistances (semilog-axis) and inductances (linear-axis) of the transformer versus reduced frequency X obtained with fine and homogenized models. The inductances are displayed in high-zoom level to show the frequency-dependence. Note that the mutual resistance is normalized by the geometric mean of the DC resistances of the primary and secondary windings.

particularly inside the litz-wire bundle, which is difficult to observe without FEA.

The impedances of the transformer are calculated from (7)-(12) via the complex power in (3). However, for the homogenized model, this is done using Z_{skin} and ν_{prox} rather than directly using (3). Fig. 10 shows the values of the resistance and the inductance from $X = 0$ to $X = 2$. The impedances obtained with the fine model and with the homogenized model are in excellent agreement. The error is less than 3% for resistance values. Although some offset errors might be seen in the inductance values, the scale level is highly zoomed and the error is less than 0.03%.

Furthermore, the increase of resistance and the slight reduction of inductance values when the frequency increases can be observed. This also illustrates the significance of mutual resistance at high frequencies. Even though from Fig. 9, the homogenized model cannot capture the fluctuation of the flux occurring in the fine model, the global values of the impedances are still correct. This obviously indicates that the homogenized model can represent the fine model of the transformer with less computational effort. This proves useful for the applications where the global results are important such as for evaluating the winding losses and for determining the inductance values to be incorporated in circuit simulators.

IV. Conclusion

A litz-wire bundle has been homogenized with the usage of a frequency-dependent complex reluctivity and a frequency-dependent complex impedance. The process has been done with the simple representative model. The results has been shown that the packing of the strands inside the bundle is not significant; only the fill factor is. As application test case a transformer with litz-wire windings has been considered. The global magnetic flux density and the impedance of the transformer calculated from the homogenized model agree excellently with the reference fine model in which each litz-wire bundle is finely discretized. The errors of the calculated resistance and inductance values are less than 3% and 0.03% respectively with several times faster calculation. This enables efficient 2-D FE model for characterizing the impedance of the litz-wire-based magnetic devices which is able to assist in the design process and circuit simulation.

Acknowledgment

This paper is part of the ADvanced Electric Powertrain Technology (ADEPT) project which is an EU funded Marie Curie ITN project, grant number 607361. Within ADEPT a virtual and hardware tool are created to assist the design and analysis of future electric propulsions. Especially within the context of the paradigm shift from fuel powered combustion engines to alternative energy sources (e.g. fuel cells, solar cells,

and batteries) in vehicles like motorbikes, cars, trucks, boats, planes. The design of these high performance, low cost and clean propulsion systems has stipulated an international cooperation of multiple disciplines such as physics, mathematics, electrical engineering, mechanical engineering and specialisms like control engineering and safety. By cooperation of these disciplines in a structured way, the ADEPT program provides a virtual research lab community from labs of European universities and industries [14]. The authors would like to thank the European Union for the funding of this research herein.

REFERENCES

[1] G. Ortiz, M. Leibl, J. W. Kolar, and O. Apeldoorn, "Medium frequency transformers for solid-state-transformer applications — Design and experimental verification," in *2013 IEEE 10th Int. Conf. Power Electron. Drive Syst.* IEEE, apr 2013, pp. 1285–1290.

[2] C. Sullivan, "Optimal choice for number of strands in a litz-wire transformer winding," *IEEE Trans. Power Electron.*, vol. 14, no. 2, pp. 283–291, mar 1999.

[3] ——, "Cost-constrained selection of strand diameter and number in a litz-wire transformer winding," *IEEE Trans. Power Electron.*, vol. 16, no. 2, pp. 281–288, mar 2001.

[4] J. Ferreira, "Analytical computation of AC resistance of round and rectangular litz wire windings," in *IEE Proc. B Electr. Power Appl.*, vol. 139, no. 1, 1992, p. 21.

[5] X. Nan and C. R. Sullivan, "An Equivalent Complex Permeability Model for Litz-Wire Windings," *IEEE Trans. Ind. Appl.*, vol. 45, no. 2, pp. 854–860, 2009.

[6] J. Gyselinck and P. Dular, "Frequency-domain homogenization of bundles of wires in 2-D magnetodynamic FE calculations," *IEEE Trans. Magn.*, vol. 41, no. 5, pp. 1416–1419, may 2005.

[7] R. V. Sabariego, P. Dular, and J. Gyselinck, "Time-domain homogenization of windings in 3-D finite element models," *IEEE Trans. Magn.*, vol. 44, no. 6, pp. 1302–1305, 2008.

[8] A. Podoltsev, I. Kucheryavaya, and B. Lebedev, "Analysis of effective resistance and eddy-current losses in multiturn winding of high-frequency magnetic components," *IEEE Trans. Magn.*, vol. 39, no. 1, pp. 539–548, 2003.

[9] D. C. Meeker, "An improved continuum skin and proximity effect model for hexagonally packed wires," *J. Comput. Appl. Math.*, vol. 236, no. 18, pp. 4635–4644, 2012.

[10] C. Geuzaine and J.-F. Remacle, "Gmsh: A 3-D finite element mesh generator with built-in pre- and post-processing facilities," *Int. J. Numer. Methods Eng.*, vol. 79, no. 11, pp. 1309–1331, sep 2009.

[11] P. Dular and C. Geuzaine, "GetDP reference manual: the documentation for GetDP, a general environment for the treatment of discrete problems." [Online]. Available: http://www.geuz.org/getdp/

[12] E. Specht, "The best known packings of equal circles in a circle." [Online]. Available: http://www.packomania.com

[13] J. H. Spreen, "Electrical terminal representation of conductor loss in transformers," pp. 424–429, 1990.

[14] A. Tamas, A. Stefanskyi, A. Dziechciarz, F. Chauvicourt, G. E. Sfakianakis, K. Ramakrishnan, K. Niyomsatian, M. Curti, N. Djukic, P. Romanazzi, S. Ayat, S. Wiedemann, W. Peng, and S. Stijpetic, "Researchers within the EU funded Marie Curie ITN project ADEPT, grant number 607361," 2013-2017.